2014 IEEE International Conference on Robotics & Automation (ICRA)
Hong Kong Convention and Exhibition Center
May 31 - June 7, 2014. Hong Kong, China

Stability of Soft-Finger Grasp under Gravity

Kensuke Harada, Tokuo Tsuji, Soichiro Uto
Natsuki Yamanobe, Kazuyuki Nagata, and Kosei Kitagaki

Abstract— **We discuss grasp stability under gravity where each finger makes soft-finger contact with an object. By clustering polygon models of a finger and an object, the contact area between a finger and an object is obtained as the common area between an object cluster and a finger cluster. Then, by assuming the Winkler elastic foundation, the pressure distribution within the contact area is obtained. By using this pressure distribution, we show that we can judge grasp stability under soft-finger contact. We further consider defining a quality measure of a soft-finger grasp by assuming that although the gravitational force is applied to an object, the direction of gravity is unknown. To demonstrate the effectiveness of the proposed approach, we show several numerical examples.**

I. INTRODUCTION

Grasp stability is widely used as an index for evaluating the grasping posture of multifingered hands. If grasp stability is satisfied, we can guarantee that the grasped object can resist an external disturbance from any direction. In this study, we focus on grasp stability for general multifingered hands, wherein a finger makes soft-finger contact (SFC) with an object. We consider solving formulating grasp stability under SFC by explicitly using the pressure distribution acting in the contact area between finger and object. In addition to this problem, we obtain the quality measure by taking the effect of gravity into consideration.

Many industrial manipulators are equipped with two-fingered parallel grippers at the tip. For such manipulators, it is well known that, if a finger contacts an object under the point contact with friction (PCwF), three fingers are needed to ensure grasp stability. However, many two-fingered grippers have a flexible sheet attached to the finger surface. When a finger contacts an object, the flexible sheet deforms, thereby generating torsional friction at the contact area. Because of this torsional friction, grasp stability can be satisfied even if a hand has only two fingers. This contact style is called SFC. Here, because the amount of torsional friction depends on the area of contact, grasp stability also depends on the area of contact. Although the area of contact depends on the object shape and the flexibility of the sheet, there has been no research on grasp stability under SFC in which the effect of object shape and flexibility of the sheet has been considered. On the other hand, we determine grasp stability under SFC by explicitly considering this effect. We assume that polygon models are given for both a finger and an object. By clustering the polygon models, we obtain the contact area as the common area between a finger cluster and an object cluster. Then, by assuming the Winkler elastic foundation[13], the pressure distribution acting at the contact area is obtained. By using the pressure distribution, we evaluate grasp stability under SFC.

Kensuke Harada, Natsuki Yamanobe, Kazuyuki Nagata and Kosei Kitagaki are with Intelligent Systems Research Institute, National Institute of Advanced Industrial Science and Technology (AIST), Tsukuba, Japan kensuke.harada@aist.go.jp

Tokuo Tsuji and Soichiro Uto are with the Faculty of Information Science and Electrical Engineering, Kyushu University, Fukuoka 819-0395, Japan tsuji@ait.kyushu-u.ac.jp

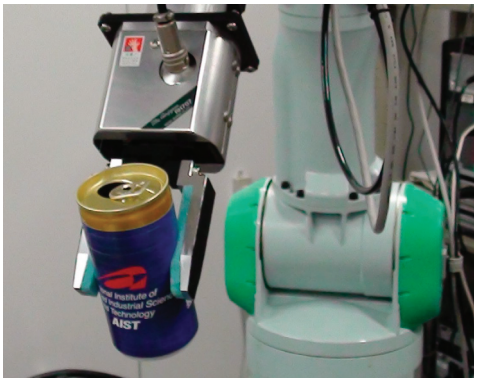

Fig. 1. Grasping a can under soft-finger contact.

For the problem of quality measure, a grasp has to be kept under gravity. Here, let us consider a situation in which a set of grasping postures is generated without knowledge of the direction of the gravitational force acting on an object before the grasp is executed. Then, an object is actually grasped by selecting one feasible grasping posture from a set of candidate postures generated in advance. To cope with this situation, the grasp quality has to be set such that a grasp is maintained under gravity while the direction of gravity is unknown. We consider a three-dimensional subset of the six-dimensional wrench set. Then, we consider a three-dimensional sphere where its radius is the same as the amount of gravitational force and whose center is located at the origin. If this sphere is included in the three-dimensional subset, we judge that grasp stability is maintained.

This paper is organized as follows: After describing some previous work in Section 2, we formulate the region of force and the moment when a finger applies a force to an object in Section 4. In Section 5, we formulate grasp stability under gravity. In Section 6, we confirm the effectiveness of the proposed approach through several numerical examples.

II. RELATED WORK

Because grasp stability is a classical robotics problem, much research has been conducted on it[1], [2], [3], [4], [5],

[6], [7], [8], [9], [10], [11], but mostly it has been assumed that a finger contacts an object under PCwF. Herem the well-known quality measure proposed by Ferrari and Canny[1] has been commonly used in many research projects. The amount of research on grasp stability under SFC however is limited. Howe and Cutkosky[12] proposed force-motion models under SFC. Ciocarlie et al.[9] examined grasp stability under SFC. However, they assumed the area of contact to be an ellipsoid of fixed size. In our previous research[14], we discussed grasp stability under SFC by approximating the contact area by an ellipsoid. Meanwhile, research on contact elasticity has a long history[13], and some researchers have tried to model the elasticity of contact when a robotic hand grasps an object[17], [18], [19].

As far as we know, ours is the first general algorithm to be developed for grasp stability under SFC, in which the effect of object shape and the flexibility of the contact have been taken into consideration.

III. DEFINITIONS

Let us consider a situation in which an object is being grasped by a multifingered hand. Let us also consider that the finger surface contacting an object is deformable, whereas the object surface is rigid. We assume that the shape of the finger contacting surface is flat when there is no deformation. Let $\boldsymbol{f}_i$ and $\boldsymbol{\tau}_i$ $(i = 1, \ldots, m)$ denote the force and moment, respectively, applied at the ith contact point of an object. τ_{ni} and $\boldsymbol{\tau}_{ti}$ denote the normal and tangential components of $\boldsymbol{\tau}_i$, respectively. For SFC, the force and moment about the contact normal are applied by a finger to an object. The wrench $\boldsymbol{\omega}$ applied to an object by all fingers is expressed by

$$\boldsymbol{\omega} = \sum_{i=1}^{m} \boldsymbol{G}_i \begin{bmatrix} \boldsymbol{f}_i \\ \tau_{ni} \end{bmatrix}, \tag{1}$$

where

$$\boldsymbol{G}_i = \begin{bmatrix} \boldsymbol{I} & 0 \\ [\boldsymbol{p}_i \times] & \boldsymbol{n}_i \end{bmatrix}$$

and $\boldsymbol{p}_i$ and $\boldsymbol{n}_i$ denote the position vector and unit normal vector of a point in the contact area, respectively.

In this research, we assume that polygon models are given for both the finger and the object. Under this assumption, we obtain the contact region on the object surface by clustering the polygon models. Let C_j $(j = 1, \ldots, n)$ be the jth cluster of the object polygon model. Also, let P_j and A_i be the plane fit to cluster C_j and the area of cluster C_j, respectively.

IV. SOFT-FINGER CONTACT

We formulate grasp stability under SFC.

A. Overview

Let μ be the static friction coefficient. We consider the case in which the relation between the contact force and the moment about the contact normal at the ith contact point can be expressed in the following form[12]:

$$\boldsymbol{f}_{ti}^t \boldsymbol{f}_{ti} + \frac{\tau_{ni}^2}{e_{ni}^2} \leq \mu^2 f_{ni}^2, \tag{2}$$

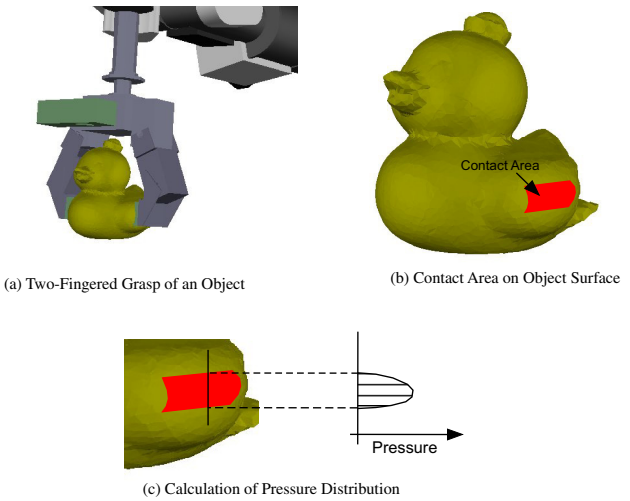

(a) Two-Fingered Grasp of an Object

(b) Contact Area on Object Surface

(c) Calculation of Pressure Distribution

Fig. 2. Calculation of pressure distribution.

where the eccentricity parameter e_{ni} of friction ellipsoid changes depending on the object shape and the area of contact. Equation (2) has to be satisfied for a multifingered hand to maintain the grasp on an object under SFC. Here, the parameter e_{ni} will be calculated in the following; an overview is roughly depicted in Fig. 2.

As shown in Fig. 2, we first consider the case where a grasping posture is given. We obtain the contact area between the finger and the object by clustering the polygon model of the object. Then, by assuming the Winler elastic foundation, the pressure distribution within the contact area is obtained depending on the amount of deformation. Once the pressure distribution is obtained, we can calculate the parameter e_{ni} by integrating the pressure distribution within the contact area.

B. Object Surface Clustering

Let us consider the situation in which a rigid object penetrates a rigid finger with a flat surface. This approximately expresses a situation in which a finger surface deforms owing to contact with an object. Let h_{max} be the penetration depth corresponding to the amount of deformation of the finger surface.

The contact region between the finger and the object can be obtained from the region on the object surface penetrated by the finger. This region can be obtained by clustering the polygon model, as explained in the following.

First, we obtain a grasping posture without taking the deformation of the finger surface into consideration. Here, $\tilde{\boldsymbol{p}}_i$ denotes the position vector of the ith grasping point. Let the tilde of cluster $\tilde{C}_j$ denote that this cluster includes the position vector $\tilde{\boldsymbol{p}}$. From an initial set of clusters, our clustering algorithm merges a neighboring cluster to cluster $\tilde{C}_j$ provided the maximum distance from the point denoted by $\tilde{\boldsymbol{p}}$ to an arbitrary point included in $\tilde{C}_j$ in the direction $\boldsymbol{n}_j$ is less than h_{max}. Among multiple neighboring clusters, we consider selecting the one whose normal vector is closest to

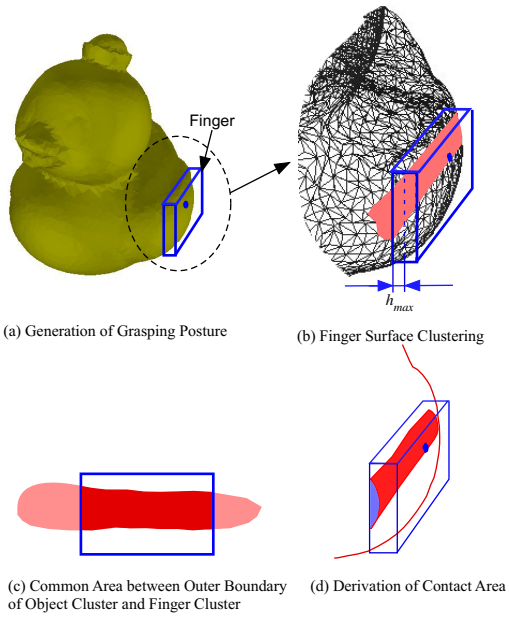

Fig. 3. Derivation of contact area based on the clustering object polygon model.

$\boldsymbol{n}_j$. This algorithm is summarized as follows:

Algorithm 1 (Object Surface Clustering)

1: while $h(\tilde{C}_j) < h_{max}$
2: $C_k \leftarrow SelectNeighborCluster(\tilde{C}_j, \boldsymbol{n}_j)$
3: $\tilde{C}_j \leftarrow \{\tilde{C}_j, C_k\}$
4: end

Here, $h(\tilde{C}_j)$ denotes the maximum distance from $\tilde{\boldsymbol{p}}$ to a point in $\tilde{C}_j$ in the direction of $\boldsymbol{n}_j$. $SelectNeighborCluster(\tilde{C}_j, \boldsymbol{n}_j)$ denotes a function to select a cluster among the neighbors of $\tilde{C}_j$ whose normal vector is closest to $\boldsymbol{n}_j$ under $h(\tilde{C}_j) < h_{max}$.

As for each finger, flat area on finger surface is limited. To obtain the boundary of flat area on finger surface, we also cluster the polygon model of each finger link contacting with an object.

After clustering the polygon model of an object, we consider obtaining the cluster's outer boundary projected onto the plane including the finger surface. The contact area on the object surface can be obtained by taking the common area between the boundary of the finger surface and the boundary of the object cluster projected onto the plane including the finger surface. We regard this common area as the contact area in this research.

C. Pressure Distribution

By using the contact area obtained in the previous subsection, we now obtain the pressure distribution within the contact area based on the Winkler elastic foundation[13]. From the Winkler elastic foundation, we can obtain a simplified model of the pressure distribution by disregarding the effect of shear stress.

As shown in Fig. 4, let us consider the coordinate system attached at the finger surface without deformation where

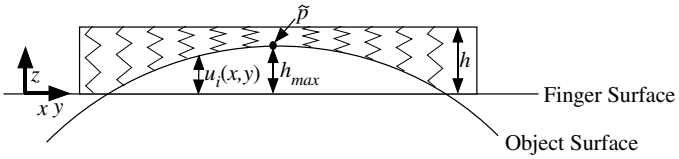

Fig. 4. Definition of deformation within the contact area.

the z-axis denotes the normal direction. Let $u_i(x, y)$ be the normal elastic displacement. The pressure distribution can be expressed as

$$p_i(x, y) = \frac{K}{h} u_i(x, y), \tag{3}$$

where K denotes the elastic modules of the foundation. From Eq. (3), the maximum tangentional force $\max(f_{ti})$ and the maximum moment $\max(\tau_{ni})$ about the contact normal acting in the contact area can be expressed as

$$\max(f_{ti}) = \int_S \mu \frac{K}{h} u_i(x, y) dS, \tag{4}$$

$$\max(\tau_{ni}) = \int_S \sqrt{x^2 + y^2} \mu \frac{K}{h} u_i(x, y) dS, \tag{5}$$

where $\int_S$ denotes the surface integral within the contact area. This surface integral is discretely calculated by using the area of the triangles included in the polygon model. From the above equations, the parameter e_{ni} shown in Eq. (2) can be calculated as[9]

$$e_{ni} = \frac{\max(\tau_{ni})}{\max(f_{ti})}. \tag{6}$$

We can now define Eq. (2) at each contact point.

V. GRASP STABILITY UNDER GRAVITY

To define the grasp wrench set (GWS), we allow Eq. (2) to act as a constraint on the force and moment at each contact point denoted as $(\boldsymbol{f}_i, \tau_{ni}) \in SFC$. It is known that there are two major definitions of the GWS: One is obtained by using the Minkowski sum and the other is obtained by the union of unit wrenches[1]. Although our grasp quality can be defined for both cases, we define the GWS by using the Minkowski sum as follows[10]:

$$W_{L^\infty}^{ch} = \left\{ \sum_{i=0}^{m} \boldsymbol{G}_i \begin{bmatrix} \boldsymbol{f}_i \\ \tau_{ni} \end{bmatrix} | (\boldsymbol{f}_i, \tau_{ni}) \in SFC,\ f_{ni} \leq f_{max} \right\}. \tag{7}$$

We now define the quality measure. As mentioned in the Introduction, we consider the situation in which grasp stability has to be maintained under gravity and the direction of gravity is unknown. Our quality measure is a modified version of Ferrari and Canny's method[1].

An overview of the proposed method is shown in Fig. 5. Let $\boldsymbol{\omega} = (\boldsymbol{\omega}_f, \boldsymbol{\omega}_\tau)$ be the six-dimensional wrench composed of a three-dimensional force and a three-dimensional moment acting on an object. Here, without loss of generality, we consider the case where the origin of the object coordinate system coincides with the center of gravity. The figure on the left-hand side shows the region of the GWS acting on

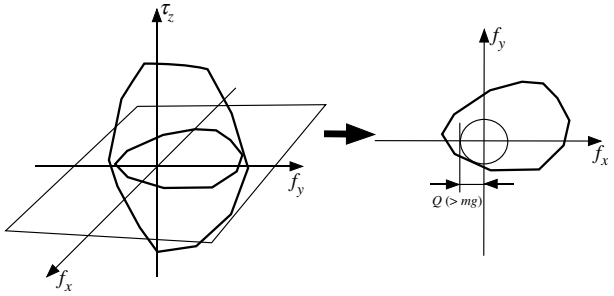

Fig. 5. Proposed method, taking the gravitational force into consideration.

an object defined by Eq. (7). We consider obtaining the following intersection:

$$W_{int} = W_{L^\infty}^{ch} \cap W_\tau, \tag{8}$$

where $W_\tau = \{\boldsymbol{\omega} | \boldsymbol{\omega}_\tau = 0\}$. We call this intersection the *GWS intersection*. In the GWS intersection, we consider a sphere whose center is located at the origin and whose radius is mg, where m is the weight of the object. If this sphere is included inside the GWS intersection, we judge that the stability is maintained. In our method, the grasp quality Q is defined as the minimum distance from the origin to the boundary of the GWS intersection. Because $Q > mg$ is always satisfied, we can guarantee that the grasp can be maintained against the gravitational force from any direction.

Here, as in many methods of grasp quality measure, the friction cone is approximated by using a convex cone[1], [9], [10]. In [9], a method involving the use of convex polyhedrons to approximate the region defined by Eq. (2) for SFC was shown. Although our method can be directly applied for Eq. (2) approximated by convex polyhedrons, we consider using a method in which the GWS is defined by a common area of multiple ellipsoids[11].

As for the quality measure obtained in this section, the conventional definition[1] does not consider the effect of object mass. Let us consider the case where a multifingered hand grasps a long bar. For this case, although we can expect that grasp is not stable if a hand grasps the edge of a bar, we need information on the object mass and the position of center of gravity to determine the grasp quality. As shown in the section of numerical examples, we will show an example of grasping a long bar by using a two-fingered parallel gripper.

VI. DISCUSSION

Our proposed algorithm of calculating the contact area becomes accurate if the polygon model is fine enough and if the effect of share stress is small enough. Here, if the effect of share stress is large, the actual contact area will be smaller than our calculation result. Hence, assuming that the approximation of friction constraint (eq.2) is accurate enough, we expect that the grasp stability obtained by our algorithm will tend to be more stable than the actual cases. The grasp stability of SFC with large share stress is considered to be our future research topic.

TABLE I

POLYGON MODELS USED IN NUMERICAL EXAMPLES

Object Name	Number of polygons
Petbottle	120698
Cell Phone	134354
Duck Toy	127162

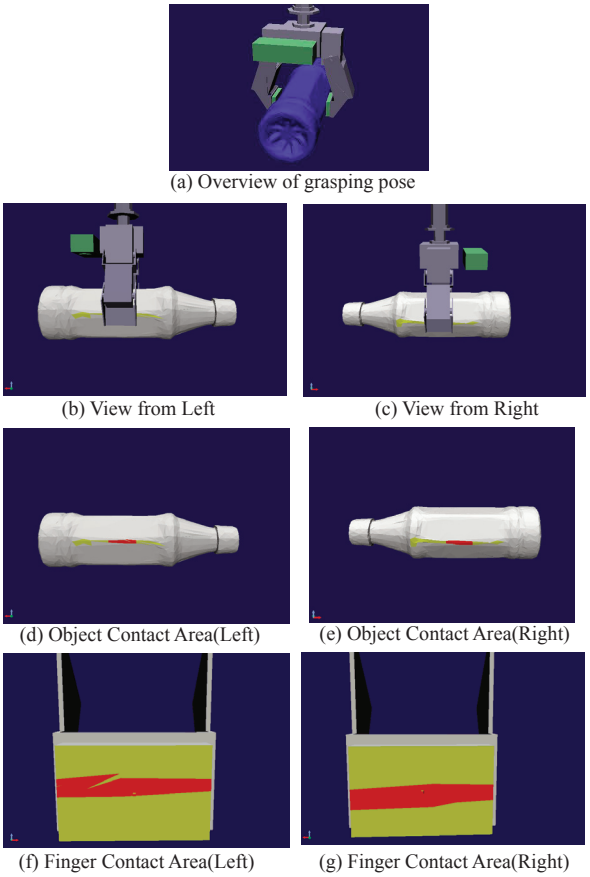

(a) Overview of grasping pose

(b) View from Left

(c) View from Right

(d) Object Contact Area(Left)

(e) Object Contact Area(Right)

(f) Finger Contact Area(Left)

(g) Finger Contact Area(Right)

Fig. 6. Example grasp of a PET bottle: 1.

Our clustering algorithm cannot deal with the case where there are two bumps on the object surface simultaneously contacting with the finger surface. This is also considered to be our future research topic.

VII. NUMERICAL EXAMPLES

To show the effectiveness of the proposed approach, we show several numerical examples. The number of polygons of object used in this section is shown in Table VII. We first calculate the contact area and e_{ni} defined in Eq. (2) for three cases. In all three cases, we set $\mu = 0.8$, $f_{max} = 15$ N, and $h_{max} = 0.001$ m. The results of our calculations are listed in Table VII. Graphics for our numerical examples are shown in Figs. 6, 7, and 8. In these figures, the yellow and red areas represent the cluster and contact areas, respectively. Although the same PET bottle is grasped, the contact area shown in Fig. 7 is larger than that shown in Fig. 6. Hence, the parameter e_n in Fig. 7 is larger than that in Fig. 6.

Next, we show an example of changing the amount of

TABLE II

CALCULATION RESULTS.

Object name	e_n (L)	e_n (R)	Contact Area (L) [m^2]	Contact Area (R) [m^2]
PET bottle: 1	6.941e-3	8.166e-3	1.267e-4	1.534e-4
PET bottle: 2	1.092e-2	1.733e-2	3.741e-4	4.714e-4
Cell phone	8.130e-3	7.661e-3	2.748e-4	1.550e-4

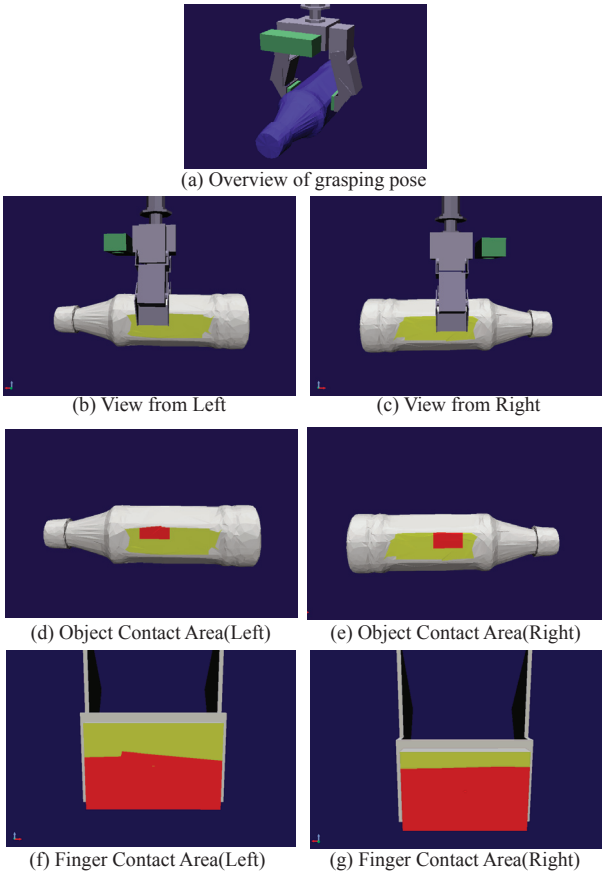

(a) Overview of grasping pose

(b) View from Left (c) View from Right

(d) Object Contact Area(Left) (e) Object Contact Area(Right)

(f) Finger Contact Area(Left) (g) Finger Contact Area(Right)

Fig. 7. Example grasp of a PET bottle: 2.

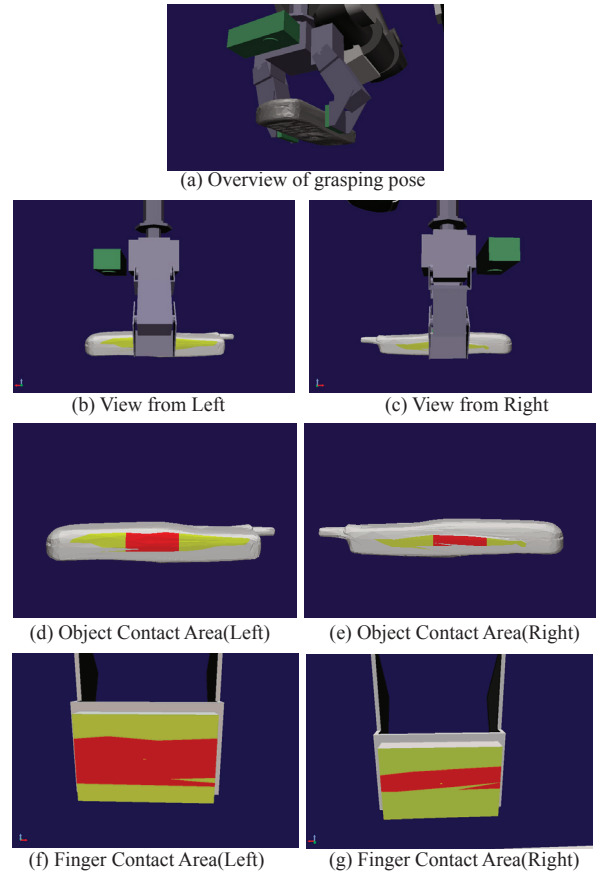

(a) Overview of grasping pose

(b) View from Left (c) View from Right

(d) Object Contact Area(Left) (e) Object Contact Area(Right)

(f) Finger Contact Area(Left) (g) Finger Contact Area(Right)

Fig. 8. Example grasp of a cell phone: 1.

deformation h_{max} and the maximum normal force f_{max}. We consider changing h_{max} in proportion to f_{max}. The result is shown in Table II and Fig. 9. As seen, as h_{max} decreases, the contact area also decreases. The quality measure also decreases and becomes unstable when $h_{max} = 0.001$ m.

We measured the calculation time needed to cluster the polygon model. By using a 3.33-GHz PC, the calculation time is about 0.26 s in all cases. This result shows that our method is practical enough to be used in most existing grasp planners.

Finally, we show the quality measure of grasping a rectangular-shaped object with a uniform mass distribution. In this example, we fixed e_{ni} to 0.1. Because of torsional friction, we can expect that the grasp to become less stable if the grasping position gets far from the center of gravity. Figure 10 shows the quality measure as a function of distance between the center of gravity and the grasping position. Because $mg = 4.9$ m/s^2, stability is satisfied when $Q > 4.9$. As shown in the figure, the grasp becomes less stable as the grasping position gets farther from the center of gravity, as we expected.

VIII. CONCLUSIONS AND FUTURE WORKS

In this paper, we proposed a method for judging grasp stability under SFC. To formulate grasp stability, we first obtained the contact area by clustering the polygon model of an object. Then, by using the Winkler elastic foundation, we defined the set of the force and the moment applied to an object by a finger. We further defined the quality measure as an intersection of the GWS and the set of zero moment. Through several numerical examples, we showed that, depending on the shape of an object and on the deformation of the finger surface, grasp stability changes. We also showed that our method is practical enough since we can obtain the grasp stability in a short period of time.

For future work, we plan to confirm the effectiveness of the proposed approach through experiments. Also, comparison

TABLE III

CALCULATION RESULTS FOR CHANGING DEFORMATION VALUES.

h_{max}	f_{max}	Q	e_n (L)	e_n (R)	Contact Area (L)	Contact Area (R)
0.005	15	8.66	6.34e-3	6.27e-3	2.59e-4	2.84e-4
0.003	9	4.31	5.34e-3	5.57e-3	1.95e-4	2.34e-4
0.001	3	0	3.43e-3	4.00e-3	9.20e-5	1.07e-4

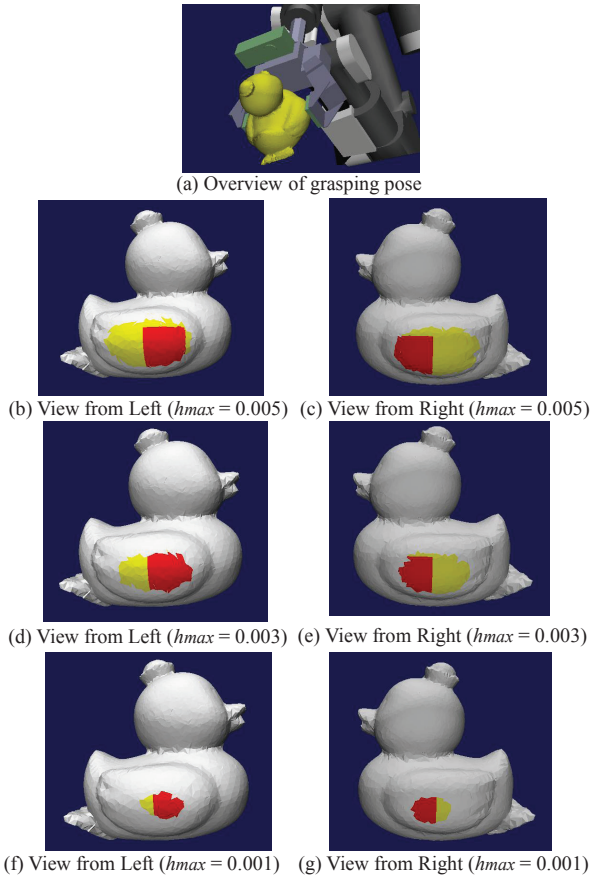

(a) Overview of grasping pose

(b) View from Left (*hmax* = 0.005) (c) View from Right (*hmax* = 0.005)

(d) View from Left (*hmax* = 0.003) (e) View from Right (*hmax* = 0.003)

(f) View from Left (*hmax* = 0.001) (g) View from Right (*hmax* = 0.001)

Fig. 9. Result of changing deformation values, where (f) and (g) show the unstable case.

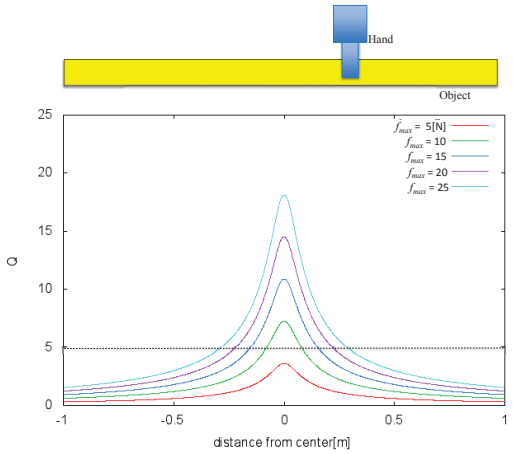

Fig. 10. Result of changing the grasping position of a rectangular-shaped object on the quality measure.

with the simulation result using finite-element method is considered to be our future research topic.

REFERENCES

[1] C. Ferrari and J. Canny, "Planning Optimal Grasps", *Proc. of IEEE Int. Conf. on Robotics and Automation*, pp. 2290-2295, 1992.

[2] A. Bicchi and V. Kumar, "Robotic Grasping and Contact: A Review", *Proc. of IEEE Int. Conf. on Robotics and Automation*, pp. 348-353, 2000.

[3] V. Nguyen, "Constructing force closure grasps", Int J Robot Res, vol. 7, no. 3, pp. 3-16, 1988.

[4] J. Ponce, D. Stam and B. Faverjon, "On Computing Twofinger Force-closure Grasps of Curved 2D Objects", Int J Robot Res, vol.12, no.3, pp.263-273, 1993.

[5] B. Mishra, N. Silver, "Some discussion of static gripping and its stability", IEEE Trans Systems, Man and Cybernetics, vol.19, no.4, pp.783-796, 1989.

[6] G.F. Liu, and Z.X. Li, "Real-time Grasping Force Optimization for Multifingered Manipulation: Theory and Experiments", IEEE/ASME Trans Mechatronics, vol.9, no.1, pp.65-77, 2004.

[7] N. Niparnan and A. Sudsang, "Positive Span of Force and Torque Components of Three-Fingered Three-Dimensional Force-Closure Grasps", *Proc. of IEEE Int. Conf. on Robotics and Automation*, pp. 4701-4706, 2007.

[8] C. Borst, M. Fischer, G. Hirzinger, "A fast and robust grasp planner for arbitrary 3D objects", *Proc. of IEEE Int. Conf. on Robotics and Automation*, vol. 3, pp.1890-1896, 1999.

[9] M. Ciocarlie, C. Lackner, and P.K Allen, "Soft Finger Model with Adaptive Contact Geometry for Grasping and Manipulation Tasks", *Proc. of World HAPTICS*, 2007.

[10] Y. Zheng, "An Efficient Algorithm for a Grasp Quality Measure", IEEE Trans. on Robotics, 2013.

[11] T. Tsuji, K. Harada, and K. Kaneko, "Easy and Fast Evaluation of Grasp Stability by using Ellipsoidal Approximation of Friction Cone", *Proc. of IEEE/RSJ Int. Conf. on Intelligent Robots and Systems*, pp.1830-1837, 2009.

[12] R.D. Howe and M.R. Cutkosky, "Practical Force-Motion Models for Sliding Manipulation", Int. J. Robotics Research, vol. 15, no. 6, pp. 557-572, 1996.

[13] K.L. Johnson, "Contact Mechanics", Cambridge University Press, 1985.

[14] K. Harada et al., "Grasp Planning for Parallel Grippers with Flexibility on its Grasping Surface", *Proc. of IEEE Int. Conf. on Robotics and Biomimetics*, pp.1540-1546, 2011.

[15] K. Harada et al., "Pick and Place Planning for Dual-Arm Manipulators", *Proc. of 2012 IEEE Int. Conf. on Robotics and Automation*, pp. 2281-2286, 2012.

[16] K. Harada et al., "Object Placement Planner for Robotic Pick and Place Tasks", *Proc. of IEEE/RSJ Int. Conf. on Intelligent Robots and Systems*, pp. 980-985, 2012.

[17] C.-H. D. Tsai, I. Kao, N. Sakamoto, M. Higashimori, M. Kaneko, "Applying Viscoelastic Contact Modeling to Grasping Task: An Experimental Case Study", *Proc. of IEEE/RSJ Int. Conf. on Intelligent Robots and Systems*, pp. 1790-1795, 2008.

[18] K. Tahara, S. Arimoto, M. Yoshida, "Dynamic Object Manipulation Using a Virtual Frame by a Triple Soft-fingered Robotic Hand", *Proc. IEEE Int. Conf. on Robotics and Automation*, pp. 4322-4327, 2010.

[19] T.Inoue and S. Hirai, "Parallel-distributed model in three-dimensional soft-fingered grasping and manipulation", *Proc. IEEE Int. Conf. on Robotics and Automation*, 2009.